Aquatic Geochemistry **6:** 435–460, 2000.
© 2000 *Kluwer Academic Publishers. Printed in the Netherlands.*

Chemical Weathering Rates, Erosion Rates and Mobility of Major and Trace Elements in a Boreal Granitic Till

MAGNUS LAND* and BJÖRN ÖHLANDER
*Division of Applied Geology, Luleå University of Technology, SE-971 87 Luleå, Sweden (*Author for correspondence. Current address: Division of Geological and Planetary Sciences, California Institute of Technology, Mail stop170-25, Pasadena CA 91125, USA.*
E-mail: magnus@maxwell.gps.caltech.edu. Fax: 626-796-9823)

(Received: 27 October 1999; accepted: 16 May 2000)

Abstract. Chemical weathering rates and erosion rates of granitic till in northern Sweden have been estimated. The present-day chemical weathering rate is compared with the long-term average weathering rate since the last deglaciation approximately 8,700 years ago. Also, the present-day release rates of major and trace elements due to chemical weathering are compared with the mobility of these elements in a spodosol profile as shown by soil water samples from the vadoze zone. The estimation of the past weathering rate is based on elemental depletion trends in a soil profile (typic haplocryod), whereas the present weathering rate is based on elemental input/output budgets in a small catchment (9.4 km^2). The long-term average chemical erosion rate, expressed as the sum of major element oxides (SiO_2, Al_2O_3, CaO, Fe_2O_3, K_2O, MgO, MnO, Na_2O, P_2O_5, TiO_2), was estimated to be 4.9 gm^{-2} yr^{-1}. The long-term base cation (Ca^{2+}, Mg^{2+}, Na^+, K^+) depletion was 0.325 keq ha^{-1} yr^{-1}. The current chemical erosion rate was estimated to be 2.4–3.0 g m^{-2} yr^{-1}, which is at least an order of magnitude higher than the rate of physical erosion, and the base cation flux due to chemical weathering is 0.356–0.553 keq ha^{-1} yr^{-1}. However, 0.074 keq ha^{-1} yr^{-1} of this flux may be related to cation exchange processes induced by atmospheric input of acid rain. There is no evidence for any recently increased weathering rate of silicates in this area. The inputs of Cd, Cu, Ni and Zn exceed the outputs, and hence, these elements are currently accumulating in the soil.

There is a distinct seasonal variation in the chemical composition of the soil water. Results from the soil water samples show that Na, followed by Si and S (Cl was not measured), are the most mobile elements in the spodosol profile between the E-horizon and the C-horizon, and that Al and Fe were the least mobile elements. However, there is no simple relationship between the mobility of an element in the spodosol profile and the current release rate due to weathering of that element. This fact may have implications for the validity of the comparison between the past and present weathering rates as performed in this study.

Key words: Weathering rates, till, spodosol, soil water, vadoze zone, mobility

1. Introduction

From an environmental point of view there are numerous reasons to study weathering, on a global scale as well as on a regional or a local scale. In fact, weathering is one of the most fundamental processes on earth, without which this planet would be very inhospitable. It has been suggested that during the last 4,000 million years, weathering has decreased the temperature at the Earth's surface by 30-45 °C (Schwartzman and Volk, 1991). This temperature decrease has been brought about through consumption of CO_2, which is a greenhouse gas, i.e., it prevents heat from radiating out of the atmosphere. Still today chemical weathering of silicates is an important mechanism for the regulation of long-term climatological conditions by consumption of CO_2 (Berner and Lasaga, 1989; Berner, 1995), and it may thus be an important factor in impeding greenhouse effects due to increased burning of fossil fuels.

Chemical weathering is also of fundamental importance for different ecosystems since many essential biochemical elements are derived from the underlying rocks (Schlesinger, 1991), and it contributes macro nutrients such as Ca, Mg, K and PO_4, as well as micronutrients such as Fe, Mn and B to the soil (White and Brantley, 1995). Not only are terrestrial ecosystems heavily dependent on chemical weathering, but the oceans are, as well (Brady and Gíslason, 1997). The dissolved solids carried by rivers entering the sea are a major source of several elements in the oceans (Whitfield, 1981, 1982; Berner and Berner, 1987).

Another important feature of chemical weathering is its ability to neutralize acids. There are several sources of acids in the environment, natural as well as anthropogenic. Natural production of acids may occur as a result of break-down of organic matter, especially in humid temperate regions where humic and fulvic substances are formed. Another natural source of acidity is carbonic acid which is formed when CO_2 dissolves in water. Due to respiration by plant roots and decomposition of organic matter, the partial pressure of CO_2 in the soil pores, and hence the concentration of H_2CO_3 in the soil water, may be considerably higher than in equilibrium with the atmosphere (Wood, 1995). Uptake of nutrient cations by plants may also increase the acidity in soils, since protons are released during the process (Sposito, 1989). However, this leads to net acidification only in cases where the plants are harvested and not returned to the soil (Karltun, 1995). Anthropogenic sources of acids also include burning of fossil fuels, whereby sulphuric and nitric oxides are emitted. Oxidation of sulphides such as pyrite and pyrhotite does also contribute sulphuric acid to the environment.

In an acidified environment the solubility and mobility of several elements are enhanced. Earlier studies have indicated that the post-industrialization weathering rate or base cation flux has increased approximately by a factor of 3 as a result of acid deposition both in Europe (Paces, 1983; Mazzarino et al., 1983) and northeastern USA (April et al., 1986). Land et al. (1999) made an attempt to compare the past long-term average weathering rate with the modern, present-day weathering

rate in the Kalix River watershed, northern Sweden. The present weathering rate of silicate minerals in terms of base cation (Ca^{2+}, Mg^{2+}, Na^{+}, K^{+}) fluxes was estimated to exceed the past weathering rate by a factor of 1.8–2.1. However, it was concluded that the data set was too limited to give any unambiguous results. Uncertainties arose due to weathering of carbonates in the Caledonian mountain range, and due to weathering of mafic minerals in locally occurring greenstones. It is therefore interesting to make a similar comparison of the past and present weathering rates in a smaller catchment, which is more homogeneous with respect to mineralogy. In this study we aim to estimate and compare the past long-term average weathering rate since deglaciation with the present-day weathering rate in a small and well-defined catchment in northern Sweden. The estimations of the past and present weathering rates are based on elemental depletion trends in soil profiles and input/output budgets for the elements in the catchment, respectively. Land et al. (1999) calculated present-day weathering rates in northern Sweden for major elements and Sr only. In this study, however, fluxes and mobilities of both major and trace elements will be considered. Also, soil water data from the vadoze zone will be discussed. The aim is to establish a measure of the mobility of various major and trace elements in a spodosol profile, and to check whether there is any relationship between this mobility and the weathering rate.

2. Study Area

The studied area is a small catchment (9.4 km^2) situated within the Kalix River watershed (Figure 1). The catchment is mainly covered by till with spodosol soil profiles (more than 90% of the area), classified as typic haplocryod according to Keys to Soil Taxonomy (Soil survey staff, 1995). Bedrock outcrops and mires add up to less than 7% of the area and there are no lakes in the catchment. The till, supporting mainly pine and spruce forest, is unsorted and consists mainly of granitic material, the principle minerals being quartz, plagioclase (An$\sim$30), K-feldspar, and biotite. Thin section studies and X-ray diffraction analysis have shown accessory amounts of amphibole, epidote, zircon, ilmenite, apatite, garnet, and clay minerals (chlorite, smectite and mixed-layer clays). In the B-horizon also Fe-oxyhydroxides ($HFeO_2 \cdot nH_2O$) is present. The bedrock in the catchment consists of a 1.8 Ga granite, and the till was deposited approximately 8,700 years ago (Lundqvist, 1986). The catchment is drained by a first-order stream called Storbergsbäcken, which is frozen during winter (December to April), the peak discharge during snowmelt in early May is about 750 l s^{-1}, and the base-flow discharge during summer and autumn is 20-30 l s^{-1}. The elevation in the catchment ranges from 110 to 375 m above sea level. The annual amount of precipitation has not been measured in the Storbergsbäcken watershed because of the difficulty of obtaining reliable data for snow. Therefore, precipitation data from three weather stations, run by the Swedish Meteorological and Hydrological Institute (SMHI), situated adjacent to the Storbergsbäcken watershed have been used. The average annual

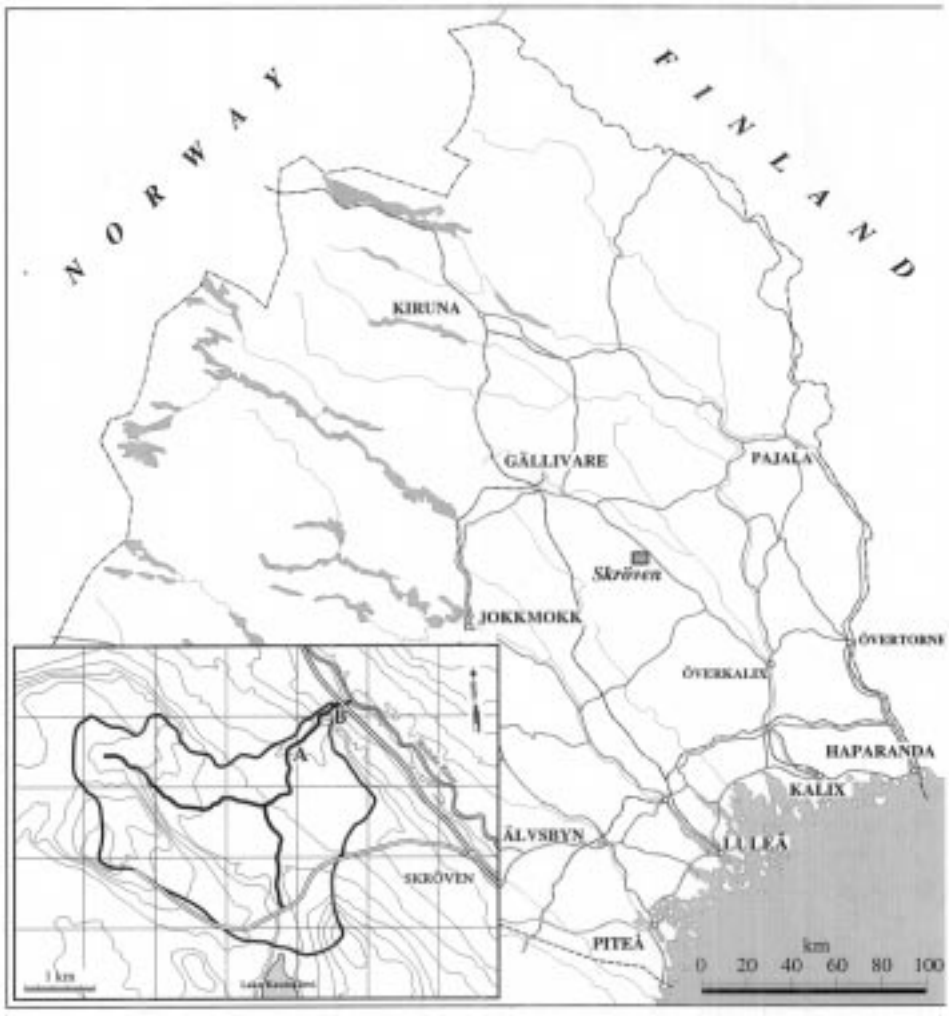

Figure 1. The Storbergsbäcken watershed. Soil, soil water and precipitation were sampled at station A. Stream water was sampled at station B.

precipitation at these stations (Pålkem, Överkalix and Korpilombolo) is 542 mm, of which approximately 250 mm evaporates (SMHI, 1996). The measured runoff in the Storbergsbäcken watershed (see below for methods) during 1994 was 247 mm. This is slightly less than the difference between average precipitation and average evaporation in this part of northern Sweden given by SMHI (1996). The annual mean air temperature is about −0.2 °C (SMHI, 1996). The sampling area is remote from any point source of pollutants and relatively uninfluenced by anthropogenic activities.

3. Sampling and Analytical Methods

In this study, soil, soil water, stream water and precipitation was sampled and analysed. On a flat horizontal site above the highest Holocene shore-line (station A, Figure 1), 19 volume-controlled (0.19–0.27 dm^3) soil samples were collected in a profile from the surface down to a depth of 130 cm. The samples were then dried and sieved and the fraction <2 mm were analysed for major elements and Ba, Be, Co, Cr, Cu, Ni, Sc, Sr, V, Zn and Zr with ICP-AES, and for Ce, Ga, Hf, Mo, Nb, Rb, Sn, Ta, Th, U, W and Y with ICP-MS after fusion with $LiBO_3$ in graphite crucibles at 1000 °C and subsequent dissolution of the fusion product in nitric acid. It is thus assumed that weathering of particles >2 mm is negligable.

Soil water was collected with cylindrical tension lysimeters (length = 95 mm, outer diameter = 21 mm) made of PTFE (polytetrafluoroethene) mixed with glass and with a pore size of 2 μm (Prenart equipment Aps., Fredriksberg, Denmark). Before installation, the PTFE cups and tubings were flushed with 1 l of 1.0 M HCl and then rinsed with 4 l of deionized water. The PTFE cups were installed horizontally from a trench (at least 0.5 m back from the trench face) at four depths; at 5 cm in the E-horizon, at 15 cm in the Bs1-horizon, at 40 cm in the Bs2-horizon, and at 100 cm in the C-horizon. A slurry of soil from the installation depths and deionized water was inserted into the holes to ensure good capillary contact between the cups and the soil. The lysimeters were connected to a tensiometer-controlled vacuum pump in such a way that the difference between the vacuum and the soil tension in the B-horizon was kept constant (-100 kPa). After installation, soil water was collected and discarded for 6 weeks. Soil water was then collected twice a month from July to November 1994, and from May to October 1995. However, the vacuum was applied continuously, i.e., each sample represents water sampled for periods of approximately two weeks. In August, no samples could be collected from the E- and Bs1-horizons due to drought. The lysimeter at 40 cm (Bs2) was working from June 1995 to October 1995 only, and is therefore not considered in this paper.

Stream water was sampled from April to November 1994, and from May to July 1995 (station B, Figure 1). The discharge was calculated on each sampling occasion after measuring water velocity and cross-sectional area in a steel canal immediately below the sampling station. A bulk composition of the winter precipitation was obtained by sampling snow cores in late April 1994, just before snowmelt. Summer precipitation was collected with a polyethylene funnel (31.5 cm in diameter) connected to a polyethylene container with a silicone tube. The funnel was mounted two metres above the ground and the container was kept in darkness to minimize biological activity in the collected water. Throughfall was collected in the same way. The stream water and precipitation (including throughfall) were immediately filtered through 0.45 μm Millipore® filters in the field and then collected in acid-leached polyethylene containers. All water samples were acidified with suprapure

HNO_3 and analysed for major ions and Sr with ICP-AES, and for trace elements with ICP-MS.

Stream water suspended matter was sampled on the same occasions as for the dissolved stream water samples by filtration through 142 mm Millipore® filters with pore size 0.45 μm. Two filters from each sampling occasion with the suspended matter were wet-ashed in concentrated nitric acid in platinum crucibles at 70°C, and then dry-ashed at 550 °C. The ashed inorganic matter was weighed, and then fused with $LiBO_2$ in graphite crucibles at 1000 °C. The beads thus formed were dissolved in 10% nitric acid and then analysed for major elements with ICP-AES, and for trace elements with ICP-MS. This procedure was also applied to filter blanks.

4. Results

4.1. PAST WEATHERING RATE IN THE STORBERGSBÄCKEN WATERSHED

The distribution of the major elements in the soil profile is shown in Figure 2. It can be seen that most of the elements are depleted in the uppermost part of the soil profile. However, it is not possible to calculate any mass changes of a certain element from the concentrations of that element alone. If the concentration of one element is changed, the concentrations of all other elements are changed as well, since the concentrations have to sum up to 100%. This leads to apparent mass changes of the other elements (e.g., the highest concentration of Si occurs in the E-horizon, although Si is in fact depleted there). One way to overcome this problem is to normalize the various element concentrations to the concentration of an immobile element which is not affected during weathering. Usually, Ti and Zr are considered to be immobile. In this work Zr is used as the normalizing element. In most silicic rocks almost all Zr occurs in the mineral zircon, $ZrSiO_4$ (Watson and Harrison, 1983), which is resistant to low-temperature weathering (Nickel, 1973; Colin et al., 1993).

Assuming that Zr is immobile during weathering, the past weathering rate may be calculated according to Equations (1) and (2),

$$\Delta m_i = \left(\frac{[i]_w [\mathrm{Zr}]_c}{[i]_c [\mathrm{Zr}]_w} - 1 \right) \tag{1}$$

$$\Delta M_i = \left(1 - \frac{[i]_c [\mathrm{Zr}]_w}{[i]_w [\mathrm{Zr}]_c} \right) [i]_w d_w \rho_w t^{-1}, \tag{2}$$

where Δm_i, and ΔM_i denote relative and absolute mass change, respectively, of element i in a weathered horizon with thickness d, ρ denotes soil density, c and w denote the C-horizon and some weathered horizon, respectively, and t is time. Square brackets refer to concentration.

The results for some of the mass change calculations are shown in Table I (major elements) and Table II (trace elements). In the calculations of the absolute mass

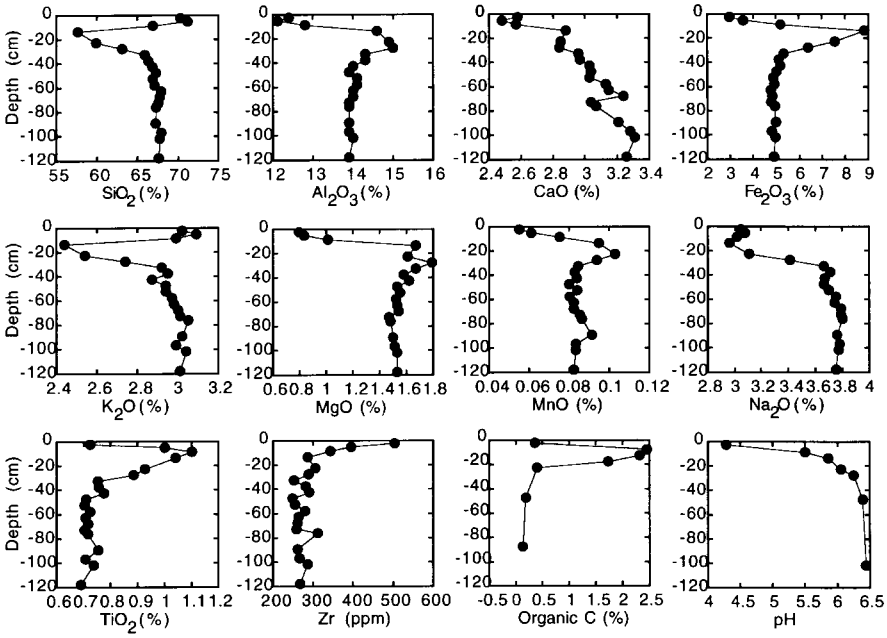

Figure 2. Distribution of major elements and of Zr, organic C and pH in the Storbergsbäcken watershed soil profile. Note the relatively large scatter for Zr.

changes it was assumed that the weathering started 8,700 years ago when the glacial ice retreated from the area. From Tables I and II it can be seen that all elements (except Hf) have been depleted in the E-horizon (0-5 cm). If the mass changes in the whole soil column (0–100 cm) are compared to the mass changes in the E-horizon, two different groups of elements can be identified. The first group consists of elements which have been depleted to a greater extent in the whole soil column than in the E-horizon only. These elements have thus been depleted also in the B-horizon. The other group consists of elements which have been more depleted in the E-horizon compared to the whole soil column. These elements have been enriched secondarily in the B-horizon. Some elements (e.g., Fe_2O_3, Table I) have been enriched in the B-horizon to a larger extent than they have been depleted in the E-horizon, i.e., there is a net mass gain for the whole soil column. Data obtained by Jersak et al. (1995) suggested that net atmospheric additions of Fe and Mn may have occurred in spodosols in northeastern USA. It is doubtful whether this is the case in the Storbergsbäcken watershed. It may alternatively demonstrate the relatively large uncertainties involved in these calculations. It should be stressed, however, that there might be real net mass gains for some of the trace elements in Table II (see Section 5.3). If the mass changes of the major element oxides are added, a chemical erosion rate of 4.9 g m^{-2} yr^{-1} is obtained. The long-term average weathering rate in terms of base cation depletion equals 0.325 keq ha^{-1} yr^{-1}.

Table I. Relative and absolute mass changes of major elements in the soil in the Storbergsbäcken watershed.

	Relative mass change, E-horizon (%)	Relative mass change, B-horizon (%)	Absolute mass change, E-horizon (mg m^{-2} yr^{-1})	Absolute mass change, 0-1000 cm (mg m^{-2} yr−1)
SiO_2	−43.3	−19.0	−2013	−3750
Al_2O_3	−55.2	−0.2	−528	−449
CaO	−64.5	−16.4	−145	−395
Fe_2O_3	−57.4	72.3	−193	240
K_2O	−45.8	−21.1	−95	−197
MgO	−74.4	4.6	−78	−81
MnO	−56.4	11.1	−3.2	−0.5
Na_2O	−59.0	−25.2	−153	−316
P_2O_5	−70.4	167	−8.8	9.6
TiO_2	−6.0	39.5	−3.0	64
LOI	145	826	73	1050

4.2. PRESENT WEATHERING RATE IN THE STORBERGSBÄCKEN WATERSHED

The basis for the calculation of the present weathering rate is Equation (3)

$$P_i + W_i + E_i = R_i + U_i, \tag{3}$$

where P is precipitation, W is weathering, E is ion exchange reactions, R is export from the catchment via rivers, U is net uptake by vegetation, and i denotes any element. Table III shows the measured concentrations in precipitation from the Storbergsbäcken watershed together with data on precipitation from the literature. Also shown in Table III are the estimated concentrations used to calculate the contribution from precipitation for each element, P_i, in the Storbergsbäcken watershed. In the calculations of P_i it was assumed that the annual precipitation is 542 mm. The results are shown in Table IV.

When the export of an element from the catchment via stream water, R_i, is calculated, both the dissolved phase and the suspended non-detrital particulate phase should be taken into account. Non-detrital suspended matter is considered as authigenic chemical precipitates and ions sorbed on these precipitates or other particles, while detrital particles are allochthonous minerals and rock fragments. The non-detrital fraction of element X (X_{nd}) in the suspended matter was determined as

$$X_{nd} = X_{meas} - (X/Ti)_{detr} Ti_{meas}, \tag{4}$$

where X_{meas} denotes the measured concentration of element X in suspended matter, Ti_{meas} denotes the measured Ti concentration in each sample, and $(X/Ti)_{detr}$

Table II. Relative and absolute mass changes of trace elements in the soil in the Storbergsbäcken watershed.

	Relative mass change, E-horizon (%)	Relative mass change, B-horizon (%)	Absolute mass change, E-horizon (μg m^{-2} yr^{-1})	Absolute mass change, 0-1000 cm (μg m^{-2} yr−1)
Ba	−49.1	−14.1	−2675	−4253
Be	−59.5	15.8	−8.2	9.6
Co	−52.3	13.3	−23.9	50.1
Cr	−73.2	20.0	−236	40
Cu	−73.7	−21.7	−61.1	554
Ga	−40.6	−29.6	−48.2	27.6
Hf	6.6	−6.2	2.3	50.5
Mo	−18.0	47.4	−1.7	14.6
Nb	−31.8	55.3	−22.2	93.5
Ni	−56.7	102	−28.5	403
Rb	−46.2	−10.2	−254	−317
Sc	−75.9	11.0	−44.7	−26.9
Sn	−41.1	−3.9	−26.2	−113
Sr	−62.5	−23.4	1260	−3058
Ta	−48.9	−10.2	−5.3	−14.6
Th	−72.1	62.7	−18	84.5
U	−69.2	−18.0	−11.6	−44.3
V	−38.0	67.9	−196	467
W	−40.9	14.6	−3.7	49.3
Y	−60.8	−3.9	−78.6	−107
Zn	−54.2	109	−115	579

denotes the element/titanium ratio for each element in detrital particles (average X/Ti ratios in till from the C-horizon). This calculation was also used by Ingri and Widerlund (1994), although they used Al as a normalizing element. The underlying assumption is that Ti is hosted in detrital particles only. When calculating the flux of elements in the stream, concentrations and discharge measured on a specific sampling occasion were considered to be valid from half the time from the previous sampling to half the time to the subsequent sampling. The calculated stream water transport of the elements in dissolved phase, non-detrital suspended phase, and total suspended phase is shown in Table IV.

The cation exchange term, E_i, in Equation (3) is very difficult to separate from the weathering term, W_i. Although difficult, it is not impossible, e.g., Åberg et al. (1989), Jacks et al. (1989) and Miller et al. (1993) showed that Sr isotopes could

Table III. Compilation of precipitation data. All values in μg l^{-1}.

	Snow. This study	Rain. This study	Through-fall. This study	Wet deposition[a]	Precipitation[b]	Precipitation[c]	Used value[e]
Ca	61	<20	348		90		**40**
Fe	6	8	30	15–32		4–22	**7**
K	<200	<200	526		98		**98**
Mg	<40	<40	98.9		24		**24**
Na	<60	<60	<60		92	110–420	<**60**
S	215	368	383			190–920	**290**
Si	<10	153[d]	613				<**10**
Al	4.20	8.55	51.7			5–44	**6.4**
As	<0.20	<0.20	<0.20	0.14–0.29			<**0.2**
Ba	0.525	0.41	4.61				**0.47**
Cd	0.022	0.054	0.056	0.07–0.17			**0.04**
Ce	<0.01	0.028	0.096				**0.02**
Co	<0.03	<0.03	<0.03				<**0.03**
Cr	1.28	<0.20	<0.20	0.13–0.19			**0.14**
Cu	<0.20	0.54	0.84	0.92–10.5			**0.37**
Hg	<0.20	<0.20	<0.20				<**0.20**
Mn	0.68	0.49	53.7	2.99–14.2			**0.58**
Mo	<0.20	<0.20	<0.20				<**0.20**
Ni	<0.30	<0.30	<0.30	0.26–0.43			**0.29**
Pb	0.574	0.44	0.78	1.40–2.45			**0.51**
Sr	<1.00	<1.00	<1.00			∼0.1	**0.1**
U	<0.01	<0.01	<0.01				<**0.01**
Yb	<0.20	<0.20	<0.20				<**0.20**
Zn	3.71	8.87	7.73	7.6–17.1			**6.3**

[a] Ross (1990). Deposition weighted averages 1988–1990, Liehittäjä, northern Sweden.
[b] Granat (1990). Deposition weighted averages 1983–1990, Pålkem, northern Sweden.
[c] Andersson (1991). Total bulk composition, 11 samples, Vettasjärvi, northern Sweden.
[d] Probable contamination from the sampling device.
[e] Estimated value for calculation of precipitation input (P_i) at Storbergsbäcken watershed. The estimated value is based on an average of concentrations in rain and snow. Litterature data has been used in cases where the concentrations were below the detection limits for both rain and snow.

Table IV. Stream water transport of elements in the dissolved load ($R(d)_i$), total suspended load ($R(\text{susp})_i$), and non-detrital suspended load ($R(nd)_i$). Nutrient net uptake (U_i), atmospheric input (P_i), and calculated weathering rates (W_i).

	$R(d)_i$ (kg yr^{-1})	$R(\text{susp})_i$ (kg yr^{-1})	$R(nd)$ (kg yr^{-1})	U_i (kg yr^{-1})	P_i (kg yr^{-1})	W_i (mg m^{-2} yr^{-1})
Ca	3828	40.9	24.4	0–2538	204	388–658
Fe	958	393	369	[a]	35	137
K	788–831	20.0	2.4	0–902	509	30.0–130
Mg	1091	13.0	6.6	0–258	102	106–133
Na	1779	17.1	0.0	[a]	<306	156–189
S	1102	17.3	17.3	[a]	1477	−38.1
Si	5301	259	35.4	[a]	<10	568
Al	187	49.2	0.0	[a]	33	16.4
P	[a]	6.5	5.9	[a]	[a]	[a]
Ti	[a]	3.2	0[b]	[a]	[a]	[a]
	$R(d)_i$ (g yr^{-1})	$R(\text{susp})_i$ (g yr^{-1})	$R(nd)_i$ (g yr^{-1})	U_i (g yr^{-1})	P_i (g yr^{-1})	W_i (μg m^{-2} yr^{-1})
Ba	7388	1139	579	[a]	2395	593
Cd	9.1-56.7	<8.4	<8.3	[a]	204	≤14.8
Ce	921	170	137	[a]	102	102
Co	123	114	107	[a]	<153	8.2–24.5
Cr	261-419	<346	<301	[a]	713	<0.7
Cu	238-499	66.9	55.4	[a]	1885	−169—141
Mn	19788	21340	20886	[a]	2955	4013
Mo	365-653	57.8	<0.1	[a]	<1020	<69.5
Ni	185-642	<35.0	<28.1	[a]	1477	≤85.8
Sr	21268	351	144	[a]	510	2224
U	110	7.7	6.0	[a]	<51	6.9–12.3
Yb	[a]	5.4	3.8	[a]	<1020	[a]
Zn	6212	<540	<511	[a]	32100	≤2700

[a] Not determined.
[b] By definition (see text).

be used for this purpose. In this study, however, cation exchange reactions, if any, are included by the weathering term.

The net nutrient uptake by vegetation, U_i, has not been estimated with any degree of certainty for the studied catchment. However, the forest in the area is old, which should mean that the uptake by growing plants and release from decaying plants have approached a steady state close to equilibrium, and that the net uptake therefore is relatively low. In the calculations of the present weathering rate two alternatives are given. The first alternative assumes that the net nutrient uptake

is zero. The other alternative assumes a net nutrient uptake as determined by the Swedish University of Agricultural Sciences (Mats Olsson, personal comm, 1995). In this case the following values for net nutrient uptake have been used: Ca^{2+} = 0.13 keq ha^{-1} yr^{-1}, Mg^{2+} = 0.023 keq ha^{-1} yr^{-1} and K^{+} = 0.024 keq ha^{-1} yr^{-1}.

The present-day weathering rate may thus be calculated as

$$W_i = R(d)_i + R(nd)_i + U_i - P_i, \tag{5}$$

where $R(d)_i$ is the dissolved load and $R(nd)_i$ is the non-detrital suspended load of element i in the stream water, respectively. The results for these calculations are given in Table IV. Considering that the area of the Storbergsbäcken watershed is 9.4 km^2, the present-day flux of base cations can be calculated to 0.356–0.553 keq ha^{-1} yr^{-1}. The uncertainties are mainly due to poorly determined net nutrient uptake by plants. If the major elements are recalculated to oxides and summed, a chemical erosion rate of 2.4–3.0 g m^{-2} yr^{-1} is obtained. This can be compared to the rate of physical erosion which can be calculated as the export of detrital matter. Using the values in Table IV and recalculate to oxides, a physical erosion rate of 0.07 g m^{-2} yr^{-1} is obtained. It can thus be concluded that the total rate of chemical erosion is at least an order of magnitude larger than the total rate of physical erosion in this system. Velbel (1985) found a similar result in another study and argued that part of the explanation could be that chemical erosion is continuous, whereas physical erosion might be more episodic and therefore not correctly sampled during sampling for particulate export.

4.3. ELEMENT CONCENTRATIONS IN SOIL WATER

The dissolved element concentrations in soil water from the vadoze zone are shown in Figure 3. The chemical composition of the soil water varied both with time and with depth. The largest temporal variations occurred in the E-horizon, while the variations in the C-horizon were relatively small. Immediately after snowmelt in May the concentrations of Ca, Mg, Na, Si and Sr were lowest in the E-horizon, probably because of dilution by meltwater, and during this time the concentrations of these elements increased with depth. Later on the concentrations started to increase in the upper horizons, resulting in roughly constant or decreasing concentrations with depth. The highest concentrations of K occurred in the E-horizon at all times. The same pattern is valid also for Fe and Al and other trace elements. For Cu there are no reliable measurements in the C-horizon. Cadmium, Cr, Mo, Ni, U and Zn could be detected in the C-horizon part of the year only. At this depth the concentrations are extremely low, which makes the data less accurate. However, the analytical precision is within 50% (2σ).

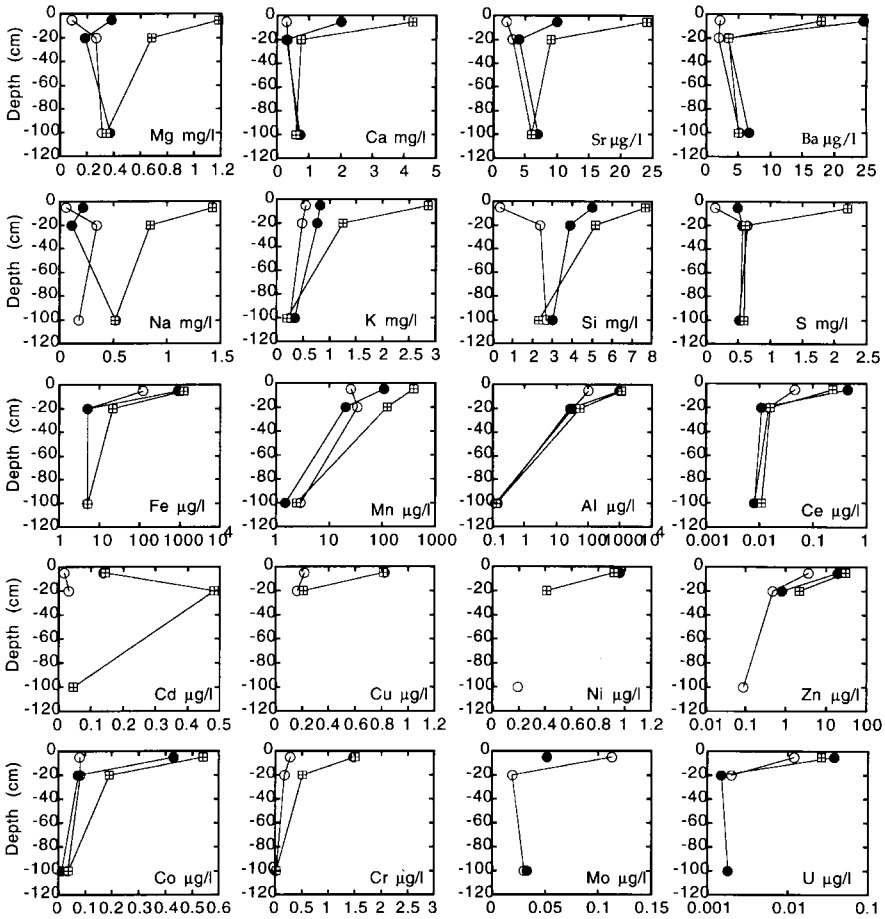

Figure 3. Dissolved element concentrations in soil water. Open circles represent May values directly after snow melt. Solid circles represent July values and squares represent October values. Note that there is a log scale for Fe, Mn, Al, Ce, Zn and U.

5. Discussion

5.1. COMPARISON OF PAST AND PRESENT WEATHERING RATES IN THE STORBERGSBÄCKEN WATERSHED

When the past and present chemical erosion rates are compared it can be seen that the total present rate is only approximately 50–60% of the past rate. Part of the explanation for this difference could be that P_2O_5 and TiO_2 are not included in the calculation of the present chemical erosion rate. However, these elements contribute only a small fraction of the total long-term average rate, and should probably be of minor importance also for the present rate. The contributions of the major elements to the past and present chemical erosion rates are shown in Table V. The present rate of chemical erosion of SiO_2, Al_2O_3, K_2O and Na_2O is lower than the

Table V. Absolute and relative contributions of the major elements to long-term average and present-day chemical erosion rates

	Past weathering rate (mg m^{-2} yr^{-1})	Present weathering rate (mg m^{-2} yr^{-1})	Past weathering rate (% of total)	Present weathering rate (% of total)
SiO_2	3750.5	1215	75.8	40.5–50.4
Al_2O_3	448.7	31.0	9.1	1.0–1.3
CaO	394.5	543–921	8.0	22.5–30.7
Fe_2O_3	−240.2	196	−4.9	6.5–8.1
K_2O	197.4	36.1–157	4.0	1.5–5.2
MgO	80.9	176–221	1.6	7.3–7.4
MnO	0.5	5.2	1.1E-2	0.2
Na_2O	316	210–255	6.4	8.5–8.7

long-term average, whereas the present chemical erosion rate of CaO and MgO is higher than the long-term average. It can also be noted that Fe_2O_3 is being depleted in the watershed at present. There is thus no evidence supporting the idea that atmospheric deposition can explain the positive mass change of Fe_2O_3 observed for the 1 m soil column in Table II (cf. Jersak et al., 1995). A more plausible explanation could be that an error is introduced when assuming that weathering of particles larger than 2 mm is negligable. If leaching of Fe from particles also larger than 2 mm takes place in the E-horizon the mass loss of Fe in that horizon is then underestimated. In the B-horizon, on the other hand, the mass gain of Fe should be correctly estimated since all the secondary Fe oxy-hydroxy precipitates are much smaller than 2 mm (although some of them appear as coatings on larger particles). This phenomenon can obviously result in an apparent smaller mass loss in the E-horizon compared to the mass gain in the B-horizon, and it would probably also apply to TiO_2 and P_2O_5.

If the weathering rates are expressed as fluxes of base cations (Ca^{2+}, Mg^{2+}, Na^+, K^+), the present rate has increased by a factor of 1.1–1.7 compared to the long-term average. The difference between the two cation fluxes, 0.031–0.228 keq ha^{-1} yr^{-1}, can be compared to the present input of sulphate to the Storbergsbäcken watershed from precipitation. The sulphate deposition amounts to 0.098 keq ha^{-1} yr^{-1}, which implies that an equal amount of acidity is introduced in the catchment. When external H^+ is added to the soil, cation exchange reactions on mineral surfaces may occur. However, as can be seen from Table IV, part of the deposited S (0.024 Keq ha^{-1} yr^{-1}, neglecting net biological uptake) is retained in the soil. This means that in order to keep a charge balance no more than 0.074 keq ha^{-1} yr^{-1} can be exchanged. The most important adsorbed cations in the soil are Ca and Mg, and it is exactly these elements that show an increased weath-

ering rate (Table V). Thus, part of the present base cation flux may be explained by cation exchange reactions in the soil due to acid deposition rather than by actual weathering of silicates. If the potential base cation flux due to ion exchange induced by atmospheric deposition of sulphuric acid is subtracted from the total present-day flux, the base cation flux due to weathering has changed by a factor 0.86–1.5 compared to the long-term average. There is thus no evidence of any recent increased weathering rate due to, e.g., changed environmental or climatological conditions. As noted above, the present chemical erosion rates of SiO_2, Al_2O_3, K_2O and Na_2O indicate that the weathering rate of silicates has actually decreased over time.

However, at this point a few problems regarding this kind of comparison of past and present weathering rates should be mentioned. First, the calculated past weathering rate is a long-term average, whereas the calculated present weathering rate is instantaneous. The instantaneous rate may increase at an early stage of the soil evolution when plants are introduced (Schwartzman and Volk, 1989, 1991; Drever, 1994), and then at a later stage decrease if, e.g., easily weathered minerals are consumed (e.g., White, 1995; White et al., 1996). If the instantaneous weathering rate changes with time, the long-term average should change with soil age. Taylor and Blum (1995) studied a soil chronosequence in the Wind River Mountains, Wyoming, and found that the long-term average weathering rate varied with time according to Equation (6),

$$R_{LT} = 215t^{-0.71}, \tag{6}$$

where R_{LT} is given in meq m^{-2} yr^{-1}, and t is time in ka. This means that even though the past and present weathering rates are found to be equal, it does not necessarily imply that the weathering rate has remained unchanged through time. According to Equation (6), the long-term average cation flux from the soil at the Storbergsbäcken watershed (8.7 ka) should be 0.46 keq ha^{-1} yr^{-1}.

Another problem with this kind of comparison is that the estimates of long-term average weathering rates usually are based on depletion trends restricted to the uppermost part of the soil, since the parent material (sediment or bedrock) at greater depths seems to be unaffected by weathering processes. In contrast, stream water discharging from a catchment has passed through much larger volumes of rocks and minerals than those present in the examined soil profiles. Minute weathering of large volumes at depth may contribute significantly to stream water chemistry. Land et al. (2000) showed that the concentrations of several elements are considerably higher in deep (25 m) groundwater hosted by bedrock compared to the concentrations in shallow groundwater hosted by till, and that this deep groundwater contributes significantly to the stream water discharge throughout the year. Furthermore, if some easily weathered mineral has been completely consumed throughout the examined soil profiles, the long-term average weathering rate will be underestimated. Several studies have concluded that calcite must contribute significantly to the release of Ca, although it could not be detected in the soil (e.g.,

Drever and Hurcomb, 1986; Mast et al., 1990). White et al. (1998) examined granitoids from several research watersheds with cathode luminescence and found trace amounts of microcrystalline calcite within silicate grains, along grain boundaries and in micro-fractures in the fresh granitoid samples. Weathered granitoid samples contained little or no observable calcite. It cannot be ruled out that calcite is also present in the fresh bedrock in the Storbergsbäcken watershed. Calcite occurring in the bedrock influences the estimate of the present weathering rate, but has no effect on the estimate of the past weathering rate. In summary: Soils better integrate time; solute budgets better integrate space (Velbel, 1993).

5.2. STREAM WATER SUSPENDED PARTICULATE MATTER

Suspended matter in streams or rivers includes both organic and inorganic components. The inorganic component may be subdivided into a detrital and a non-detrital component. If Ti is assumed to be hosted by detrital matter only, the mass of non-detrital matter may be calculated according to Equation (7),

$$m_{\text{non-dir}} = m_{\text{total}} - \frac{m_{\text{Ti}}}{C_{\text{dir}}^{\text{Ti}}}, \tag{7}$$

where m is mass and C is concentration (the non-detrital fraction of a particular element may be calculated according to Equation (4)). It should be kept in mind, however, that the assumption that Ti occurs only in detrital particles may not be valid since Ti has been mobile during weathering in the E-horizon (Table I). Another problem with Ti normalization is the possibility of mechanical sorting of the suspended matter, since Ti may be concentrated in heavy minerals. If these minerals are preferentially transported along the stream bed they are not sampled representatively, and that would result in an over-estimation of the non-detrital fraction. The same problems are associated with Equation (4), and thus also the results shown in Table IV. However, if Al is used instead of Ti, almost exactly the same results are obtained. Mechanical sorting does not seem to be a major problem in this case.

The total amount of suspended matter in the Storbergsbäcken stream is shown in Figure 4. At the beginning of the snowmelt the load of suspended matter increased, whereafter it decreased. During summer the load was temporarily increased again. If the suspended matter is divided into a detrital and a non-detrital component it can be seen that it was the detrital component that contributed to the increased load during spring flood (Figure 5a). The load of the non-detrital component decreased rapidly during spring flood. During summer the load of the detrital component was low and fairly constant. At this time it was instead the non-detrital phase that contributed to the temporary increase of the total suspended load. The non-detrital component dominated by far the load of inorganic suspended matter except for periods of high discharge during spring flood (Figure 5b). However, at these high discharge events relatively large amounts of suspended matter were transported in

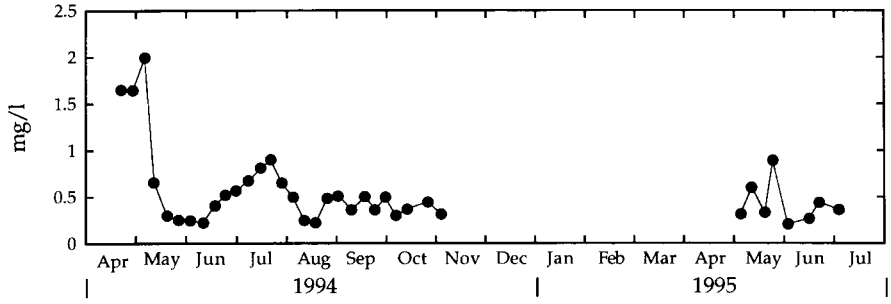

Figure 4. Total suspended load in the Storbergsbäcken Stream.

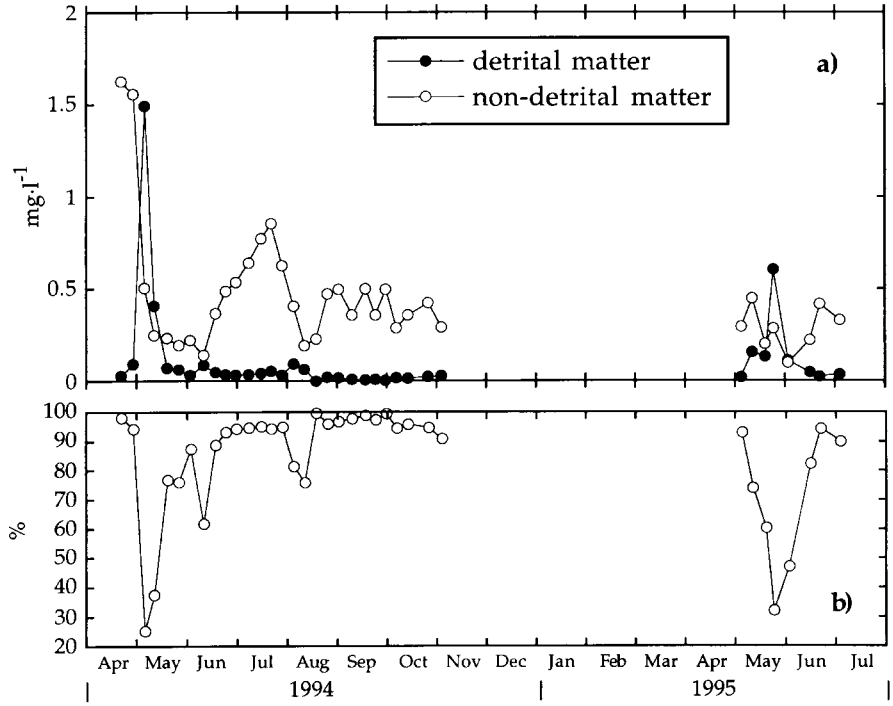

Figure 5. (a) Detrital and non-detrital suspended load in the Storbersbäcken Stream. During high discharge at snowmelt seasons, the increased total suspended load was caused by an increase in the detrital load. During summer the non-detrital load was responsible for the total increase. (b) Non-detrital fraction of total suspended load (decreasing at high discharge). The stream water is frozen December to April.

the stream, resulting in about equal proportions of discharged detrital and non-detrital inorganic matter over an annual cycle (51% non-detrital matter). The major components of the non-detrital suspended matter were Fe_2O_3 (73.2% on average), SiO_2 (10.5% on average), CaO (4.7% on average) and MnO_2 (4.6% on average).

The non-detrital phase dominated the particulate transport of Fe, Mn and P in the stream water (Table IV). More than 90% of the particulate transport of these

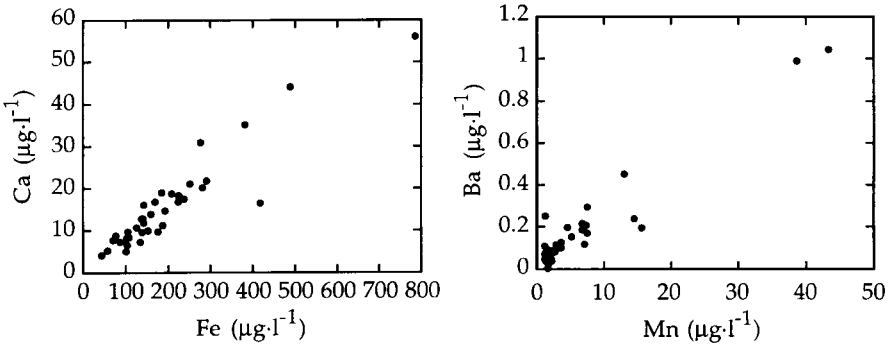

Figure 6. Non-detrital Ca and Ba vs. non-detrital Fe and non-detrital Mn, respectively.

elements was associated with the non-detrital fraction. Approximately 60 and 50% of the particulate transport of Ca and Mg, respectively, occurred in non-detrital particles, whereas less than 15% of particulate Si, Al, Na and K resided in the non-detrital material. Ingri and Widerlund (1994) showed that Ca, Mg, Sr, Ba and to a certain extent also Na and K were adsorbed on authigenic (non-detrital) Fe particles in the Kalix River. They showed also that Ba was adsorbed on authigenic Mn particles to a larger extent than the other elements. In the Storbergsbäcken stream there also seem to be positive correlations between the non-detrital Fe and the alkaline earth metals (Figure 6). Barium seems to be scavenged by Mn particles more effectively than by Fe particles.

These data show that even though the chemical erosion rate is much higher than the physical erosion rate, particulate transport may be very important for the export of certain elements, such as Fe and Mn, to the ocean. For these elements the particulate transport accounted for 29% and 52%, respectively, of the total export. However, compared to the world average river transport (Martin and Meybeck, 1979), the particulate transport in the Storbergsbäcken stream is less important. An enhanced importance of the dissolved load has also been observed for some polluted rivers (Salomons and Förstner, 1984), but in this case it probably just reflect the very low suspended load compared to the world average. The same conclusion was made by Yeats and Bewers (1982) for the St. Lawrence River in Canada.

5.3. TRACE ELEMENT MASS BALANCES

Table II indicates that several trace elements have a positive mass change in the 1 metre soil column, i.e., a negative long-term average weathering rate. One explanation for this could be that the method used to calculate the mass changes is marred by relatively large uncertainties and errors, as was probably the case for Fe. However, taking a look at Table IV, it can be seen that the present-day atmospheric inputs of Cd, Cu, Ni and Zn are considerable higher than the outputs through stream water. The input of Cr almost balances the output. Negative long-term average

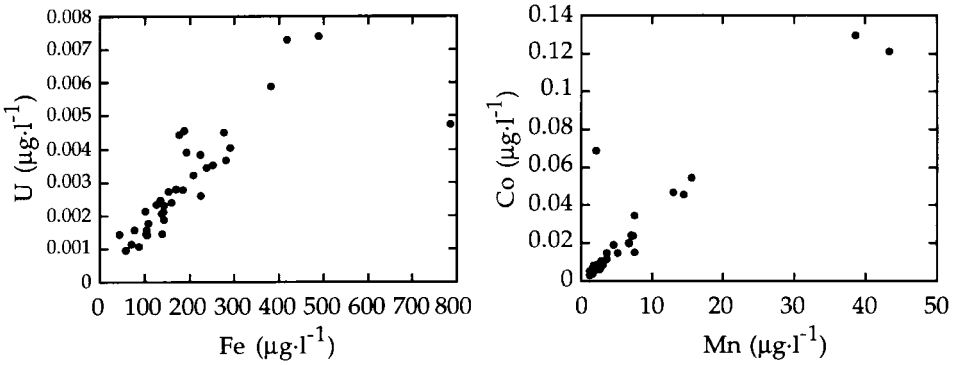

Figure 7. Non-detrital U and Co vs. non-detrital Fe and non-detrital Mn, respectively.

weathering rates for these elements seem thus not unrealistic. In another study, Aastrup et al. (1996) studied trace metal balances for seven different catchments located in both northern and southern Sweden, and found that the export of Cu exceeded the import in only one of these catchments. The export of Zn exceeded the import in three catchments, all of which were acidified and located in southern Sweden. They also found that the mobility of Cd was more sensitive to the soil pH than were Cu and Zn. The accumulation of trace metals in the Storbergsbäcken watershed soil seems to occur in the spodic B-horizon, and also in the C-horizon (see Section 5.4). Other trace elements, such as Ba, Sr, Co, Mo, Ce and U show positive weathering rates, i.e., these elements are being depleted in the watershed.

From Table IV it is obvious that a large fraction of several trace metals in stream water suspended particulate matter is transported in the non-detrital phase. More than 80% of the particulate Ce and Cu, and as much as 93% of the particulate Co, resided in the non-detrital phase. In contrast, the non-detrital fraction is insignificant for Mo, which when dissolved in neutral to moderately alkaline fresh water probably is present as the negatively charged molybdate (MoO_4^{2-}) ion (Landergren and Manheim, 1978). For Cd, Cr, Ni and Zn there are some uncertainties because of high background concentrations in the filter blanks. The average blank ($n = 4$) contained 0.013, 1.0, 0.088 and 0.60 μg of Cd, Cr, Ni and Zn, respectively, whereas the average sample (n=35) contained 0.032, 1.24, 0.12 and 1.70 μg, respectively. The blank values have not been subtracted from the particulate transport in Table IV, but the numbers are instead given as maximum values. In Figure 7 the amounts of non-detrital U are plotted as a function of non-detrital Fe. As was the case for Ba, Co was more strongly scavenged by secondary Mn particles (Figure 7). However, for the total export of the trace metals given in Table IV the particulate phase is most significant for Co (48.1%) and Cu (21.9%).

5.4. MOBILITY OF MAJOR AND TRACE ELEMENTS IN THE SPODOSOL SOIL PROFILE

Looking at dissolved alkali metals and alkaline earth metals in the soil water (Figure 3), it can be seen that in May the lowest concentrations of Na, Ca, Mg and Sr occur in the E-horizon. In July the lowest concentrations occur in the B-horizon, and in October the lowest concentrations occur in the C-horizon. Also, the concentrations in the B-horizon are generally lower in July compared to May and October, and the concentrations in the C-horizon are slightly lower in October than in July. Thus, the situation can be viewed upon as if a pulse of dilute melt water is percolating down the soil column while progressively getting more concentrated. At a depth of one metre the concentrations have reached a level where the seasonal variations are very small. In the E-horizon it can be seen that the concentrations increase with time. This increase may be promoted by weathering, ion exchange or evapotranspiration processes, but unfortunately, at present there are no data making it possible to separate these processes available.

Potassium and Ba deviate from the behaviour of the other measured alkali metals and alkaline earth metals. The concentrations of K are at all times decreasing with depth, resulting in lowest concentrations in the C-horizon. If the concentrations of K and Na in the E-horizon are compared the concentrations of K are remarkably high. Although the concentrations of these elements in the till are equal (3.0% in the E-horizon), and although most of the K is likely to reside in K-feldspar, which is rather resistant to weathering compared to plagioclase, the concentrations of K in the soil water are 2–10 times higher than the Na concentration. However, the dissolved K/Na ratio in the E-horizon decreases with time from May to October. These data suggest that there is an extensive biological cycling of K in the soil: during snowmelt large amounts of K are released from decaying organic matter in the organic and humic soil horizons, and when the K has moved down to the mineral soil it is taken up by plants. As the growing season proceeds the K/Na ratio in the E-horizon decreases which may be resulting from a combination of biological uptake of K and a faster weathering rate of plagioclase compared to K-feldspar. The lowest concentrations of Ba occur in the B-horizon at all times. This is probably due to adsorbtion processes. Nesbitt et al. (1980) found in a weathering profile of a granodiorite that Ba was retained on clays to a much larger degree than Ca and Sr. Also, the Ba/Sr ratios in the Storbergsbäcken watershed was discussed by Land et al. (2000). Below the B-horizon the Ba concentrations increase which suggests that weathering/ion exchange processes or evapotranspiration processes occur at this depth, and that the uptake and biological cycling of Ba is not as important as it is for K.

The temporal and spatial variations of dissolved Si in the soil water resemble those of Na, Ca, Mg and Sr. Berner et al. (1998) showed data on dissolved Ca, Mg, Na, K and Si in soil water from a sandbox experiment at Hubbard Brook, New Hamphsire, U.S.A., and suggested that changing temperature was the lead-

ing cause of the seasonal variations in the concentrations of these elements. This relationship can not be seen in the Storbergsbäcken watershed. Rather, the main factors controlling the concentrations of these elements appear to be contact time with the soil and/or evapotranspiration effects. For K biological uptake and cycling also seem to be important. An important difference between Hubbard Brook and Storbergsbäcken is the permeability of the two soils, and this might explain the different results. The Hubbard Brook soils were highly permeable, while the (saturated) hydraulic conductivity of the Storbergbäcken soil is rather low ($\sim 10^{-6}$ m/s). Also, the soil at Hubbard Brook was transported, disturbed and then placed in the sandboxes, while at Storbergsbäcken the soil water was sampled from a fairly undisturbed natural system.

Very high dissolved concentrations of Fe, Mn and Al was observed in the E-horizon. These high concentrations were sustained by a low pH (Figure 2) and high concentrations of complexing organic acids (no data shown). As the water percolates through the soil the pH increases and the organic complexes break down, resulting in a much lesser solubility of Fe, Mn and Al. Thus, in the B-horizon these elements precipitate and form secondary oxy-hydroxides and clay minerals. From Figure 2 it is also evident that organic matter (organic C) has accumulated in the B-horizon. These reactions are typical for podzolization. Note also that Mn appears to be more mobile further down in the soil compared with Fe and Al. The lowest concentrations of Fe, Al and Mn always occur in the C-horizon.

Other trace metals in the soil water show essentially the same pattern as Fe and Al, and it is likely that these trace elements are coprecipitated and/or adsorbed on the Fe and Al precipitates. Clay minerals and organic matter (humic and fulvic substances) may also trap the trace metals. One way to measure the mobilities of the various elements in the soil is to measure the mass gains or losses of the dissolved elements in the soil water as it flows through the soil. However, to account for evapotranspiration processes the concentrations have to be normalized to some conservative constituent. Thus, if it is assumed that the porosity (p) is constant with soil depth, the mass change of element i can be calculated according to Equation (6),

$$\Delta m_i = C_i^e\{t_0\} p \phi_e\{t_0\} (\eta - 1), \tag{8}$$

where the enrichment factor, η, is calculated as

$$\eta = \frac{C_i^c\{t_0\} C_k^e\{t_0\}}{C_i^e\{t_0\} C_k^c\{t\}}, \tag{9}$$

and where C is concentration, k denotes some conservative element, ϕ is water saturation and e and c denote the E-horizon and C-horizon, respectively. The water is assumed to enter the soil at time t_0 and to reach the C-horizon at time t. Assuming that the concentrations in the E-horizon in May (at time t_0) are the starting concentrations, and that the concentrations in the C-horizon in October (at time t) are the

Table VI. Elemental mobilities in the spodosol profile calculated according to Equation (9) neglecting evapotranspiration effects (η), and current weathering rates normalized to the abundance in the soil (W_i/m_i).

Element	η	W_i/m_i (yr^{-1} 10^6)	Element	η	W_i/m_i (yr^{-1} 10^6)
Na	>8.5	5.6–6.8	K	0.37	1.2–5.1
Si	6.5	1.75	Mo	0.28	<37
S	4.2	[a]	Ce	0.24	2.0
Mg	4.0	11–14	U	0.15	2.7–4.8
Sr	3.0	6.6	Mn	0.10	4.5
Cd	2.7	<0	Cr	0.07	<0.01
Ba	2.3	0.6	Zn	0.02	< −60
Ca	2.0	17–29	Fe	<0.04	3.5
Co	0.48	0.9–2.8	Al	0.001	0.2

[a] Not determined.

final concentrations, the mass changes in the dissolved phase may be calculated. We have no data on any conservative element, but if evapotranspiration effects are neglected (i.e., asumming that $C_k^e\{t_0\}/C_k^c\{t\} = 1$), the relative mobilities of the elements may be estimated. Since the seasonal variation in the concentrations of the non-conservative elements in the C-horizon is very small, the choice of t makes little difference in these estimations. The calculated η values are shown in Table VI. The most mobile element through the 1 m spodosol profile between the E-horizon and the C-horizon is Na, followed by Si and S, whereas Fe and Al are the least mobile elements. However, it should be remembered that these calculations are based on the simplified situation where a pulse of meltwater is moving in a plug-flow manner down the soil column. In reality, the flow through the soil is much more complex.

The mobility of Cd is remarkably high, approximately two orders of magnitude higher than that of Zn. In fact, Cd appears to be even slightly more mobile than Ca. Considering that Cd shows a negative weathering rate (Table IV), this element should be accumulating somewhere else, either below or above the investigated mineral soil column. Among the studied elements, Cd is unique in the sense that it is the only element that substantially and consistantly throughout the year shows lower concentrations in the E-horizon compared to the precipitation. This indicates that Cd is strongly retained by the overlying humic layer. However, there are no chemical data on the humic matter available to confirm this. The other trace metals showing negative weathering rates, i.e., Cu, Zn and Ni are more likely to be accumulating in the B- and C-horizons. For dissolved Cu there are no reliable measurements in the C-horizon, but preliminary results from a sequential extraction study show that particulate Cu is mainly associated with amorphous Fe-hydroxides, and in the B-horizon also organic matter.

An interesting point is that the mobility of Cd through the uppermost metre of the mineral soil is several orders of magnitude higher than that of Fe and Al, and yet Cd shows a negative weathering rate whereas Fe and Al both show positive weathering rates. This highlights the importance of surficial soil water during stream water generation. In order to export significant amounts of dissolved Fe and Al from the Storbergsbäcken watershed, an appreciable amount of soil water from the E-horizon must contribute to the stream water without passing the rest of the soil profile. Groundwater contains less than 0.03 mg l^{-1} of Fe, whereas the Fe concentration in stream water ranges between 0.38 and 1.5 mg l^{-1} (Land and Öhlander, 1997). The importance of soil water in this context was also discussed by Land et al. (2000). However, the soil water from the E-horizon is depleted rather than enriched in Cd. It can also be observed that despite that the highest release rate due to weathering (in relation to the total amount present in the soil) is shown by Ca, the mobility of this element is only moderately high (Table VI). Hence, it may be concluded that there is no simple, straight forward relationship between the mobility of an element in the spodosol profile (η_i) and the current weathering rate (W_i) of that element. This result may have implications for the validity of the method used in this study to compare the past and present weathering rates. Further research is needed.

6. Conclusion

A major conclusion in this study is that there is no evidence for any increased weathering rate of silicates in granitic till in northern Sweden as a result of, e.g., changed environmental conditions. The present-day rate of chemical erosion is 2.4–3.0 gm^{-2} yr^{-1}, or 50–60% of the long-term average chemical erosion rate which is 4.9 g m^{-2} yr^{-1}. This indicate that the chemical weathering rate has actually decreased over time. On the other hand, the present flux of Ca and Mg ions seems to have increased compared to the long-term average. The present and long-term average fluxes of base cations are 0.356–0.553 keq ha^{-1} yr^{-1} and 0.325 keq ha^{-1} yr^{-1}, respectively. After correction for potential contributions from cation exchange reactions due to present-day deposition of sulphuric acids (0.074 keq ha^{-1} yr^{-1}), the cation flux from weathering has changed by factor of 0.86–1.5.

It is also concluded that the chemical erosion rate is at least an order of magnitude higher than the rate of physical erosion in the studied area. However, for some elements (e.g., Fe, Mn, Co, Cu) the particulate phase is very important for the transport to the sea. The major part of these elements in the particulate phase were associated with secondary, non-detrital particles. In this case it means that they were probably leached into solution and then precipitated or adsorbed on secondary Fe or Mn precipitates or other particles.

Another conclusion is that Cd, Cu, Ni and Zn appear to be accumulating in the soil in northern Sweden, i.e., the input exceeds the output. Cadmium seems at least

in part to be retained in the humic layer overlying the mineral soil, whereas Cu, Ni and Zn is more likely to accumulate in the B- and C-horizons in the soil. The mobility of the major and some trace elements through the soil from the E-horizon to the C-horizon decrease in the order Na > Si > S > Mg > Sr > Cd > Ba > Ca > Co > K > Mo > Ce > U > Mn > Cr > Zn > Fe > Al. The mobility of Cd through this soil section is comparable to that of Ca, and two orders of magnitude higher than that of Zn. There is no obvious relation between the mobility of the various elements in the soil and the release rate due to weathering.

Acknowledgements

This work was supported by a research grant provided by the Swedish Geological Survey. The chemical analyses of the samples were performed at SGAB Analytica, Luleå, Sweden. The paper benefited from the valuable comments by S. R. Gíslason and an anonymous reviewer.

References

Aastrup, M., Bringmark, L., Bråkenhielm, S., Hultberg, H., Iverfeldt, Å., Kvarnäs, H., Liu, Q., Löfgren, S. and Thunholm, B. (1996) *Impact of Air Pollutants on Processes in Small Catchments, Integrated Monitoring 1982–1995 in Sweden.* Swedish Environmental Protection Agency, Report 4524.

Åberg, G., Jacks, G. and Hamilton, P. J. (1989) Weathering rates and $^{87}Sr/^{86}Sr$ ratios: An isotopic approach. *J. Hydrol.* **109**, 65–78.

Andersson, P., Ingri, J. and Boström, K. (1991) Manganese in rain, throughfall and riverwater in north Swedish coniferous forest. In *Hydrogeochemistry of Iron, Manganese, and Sulphur- and Strontium Isotopes in a Coniferous Catchment, Central Sweden.* Dissertation P. Andersson, Stockholm University. ISBN 91-7146-884-6.

April, R., Newton, R. and Truettner Coles, L. (1986) Chemical weathering in two Adirondack watersheds: Past and present-day rates. *Geol. Soc. of Am. Bull.* **97**, 1232–1238.

Berner, R. A. (1995) Chemical weathering and its effect on atmospheric CO_2 and climate. In *Chemical Weathering Rates of Silicate Minerals* (eds. A. F. White and S. L. Brantley), pp. 565–583. *Reviews in Mineralogy*, Vol. 31. Mineralogical Society of America, Washington D.C.

Berner, E. K. and Berner, R. A. (1987) *The Global Water Cycle*. Prentice-Hall, New Jersey.

Berner, R. A. and Lasaga, A. C. (1989) Modeling the geochemical carbon cycle. *Scientific American.*

Berner, R. A., Rao, J.-L., Chang, S., O'Brien, R. and Keller, K. (1998) Seasonal variability of adsorption and exchange equilibria in soil waters. *Aquatic Geochem.* **4**, 273–290.

Brady, P. V. and Gíslason, S. R. (1997) Seafloor weathering controls on atmospheric CO_2 and global climate. *Geochim. Cosmochim. Acta* **61**, 965–997.

Colin, F., Alarçon, C. and Vieillard, P. (1993) Zircon: An immobile index in soils? *Chem. Geol.* **107**, 273–276.

Drever, J. I. (1994) The effect of land plants on weathering rates of silicate minerals. *Geochim. Cosmochim. Acta* **58**, 2325–2332.

Drever, J. I. and Hurcomb, D.R. (1986) Neutralization of atmospheric acidity by chemical weathering in an alpine drainage basin in the North Cascade Mountains. *Geology* **14**, 221–224.

Granat, L. (1990) *Luft- och nederbördskemiska stationsnätet inom PMK.* Swedish Environmental Protection Agency, Report 3942 (in Swedish).

Ingri, J. and Widerlund, A. (1994) Uptake of alkali and alkaline earth elements on suspended iron and manganese in the Kalix River, northern Sweden. *Geochim. Cosmochim. Acta* **58**, 5433–5442.

Jacks, G., Åberg, G. and Hamilton, P. J. (1989) Calcium budgets for catchments as interpreted by strontium isotopes. *Nord. Hydrol.* **20**, 85–96.

Jersak J., Amundson R. and Brimhall G., Jr. (1995) A mass balance analysis of podzolization: Examples from the northeastern United States. *Geoderma* **66**, 15–42.

Karltun, E. (1995) Soil acidification – general concepts. In *Acidification of Forest Soils on Glacial Till in Sweden* (ed E. Karltun), pp. 11–14. Swedish Environmental Protection Agency, Report 4427.

Land, M. and Öhlander, B. (1997) Seasonal variations in the geochemistry of shallow groundwater hosted by granitic till. *Chem. Geol.* **143**, 205–216.

Land M., Ingri J. and Öhlander B. (1999) Past and present weathering rates in northern Sweden. *Appl. Geochem*. **14**, 761–774.

Land, M., Ingri, J., Andersson, P.S., Öhlander, B. (2000) Ba/Sr, Ca/Sr and $^{87}Sr/^{86}Sr$ ratios in soil water and groundwater: implications for relative contributions to stream water discharge. *Appl. Geochem.* **15**, 311–325.

Landergren, S. and Manheim, F. T. (1978). Molybdenum. In *Handbook of Geochemistry* (ed. K. H. Wedepohl), Vol. II(4), pp. 42H1–42H5. Springer Verlag, Berlin.

Lundqvist, J. (1986) Late Weichselian glaciation and deglaciation in Scandinavia. In (eds. V. Sibrava, D. Q. Bowen and G. M. Richmond), *Quaternary Glaciations in the Northern Hemisphere. Quaternary Sci. Rev.* **5**, 269–292.

Martin, J.-M. and Meybeck, M. (1979) Elemental mass-balance of material carried by major world rivers. *Marine Chem.* **7**, 173–206.

Mazzarino, M. J., Heinrichs, H. and Fölster, H. (1983) Holocene versus accelerated actual proton consumption in German forest soils. In *Effects of Accumulation of Air Pollutants in Forest Ecosystems* (eds. B. Ulrich and J. Pankrath), pp. 113–123. D. Reidel Publishing.

Mast, M. A., Drever, J. I. and Baron, J. (1990) Chemical weathering in the Loch Vale Watershed, Rocky Mountain National Park, Colorado. *Water Resources Res.* **26**, 2971–2978.

Miller, E. K., Blum, J. D. and Friedland, A. J. (1993) Determination of soil exchangeable-cation loss and weathering rates using Sr isotopes. *Nature* **362**, 438–441.

Nesbitt, H. W., Markovics, G. and Price, R. C. (1980) Chemical processes affecting alkalis and alkaline earths during continental weathering. *Geochim. Cosmochim. Acta* **44**, 1659–1666.

Nickel, E. (1973) Experimental sissolotion of light and heavy minerals in comparison with weathering and intrastitial solution. *Contrib. in Sediment.* **1**, 1–68.

Paces, T. (1983) Rate constants of dissolution derived from the measurements of mass balance in hydrological catchments. *Geochim. Cosmochim. Acta* **47**, 1855–1864.

Ross, H. (1990) *Övervakning av tungmetallhalter i nederbörden.* Swedish Environmental Protection Agency, Report 3943 (in Swedish).

Salomons, W. and Förstner, U. (1984) *Metals in the Hydrocycle*. Springer-Verlag, Berlin.

Schlesinger, W. H. (1991) *Biogeochemistry, an Analysis of Global Change.* Academic Press, San Diego.

Schwartzman, D. and Volk, T. (1989) Biotic enhancement of weathering and the habitability of Earth. *Nature* **340**, 457–460.

Schwartzman, D. and Volk, T. (1991) When soil cooled the world. *New Scientist*.

Soil Survey Staff (1995) *Keys to Soil Taxonomy*, 5th edn. SSMS technical monograph No. 19. Pocahontas Press, Inc., Blacksburg, Virginia, 556 pp.

Sposito, G. (1989) *The Chemistry of Soils*. Oxford University Press, Oxford.

Swedish Meteorologic and Hydrologic Institute, SMHI (1996) Väder och vatten. En tidning från SMHI -Väderåret 1995. Norrköping: Swedish Meteorological and Hydrological Institute. ISSN 0281-9619 (in Swedish).

Taylor, A. and Blum, J. D. (1995) Relation between soil age and silicate weathering rates determined from the chemical evolution of a glacial chronosequence. *Geology* **23**, 979–982.

Velbel, M. A. (1993) Weathering and pedogenesis at the watershed scale: Some recent lessons from studies of acid-deposition effects. *Chem. Geol.* **107**, 337–339.

Watson, E. B. and Harrison, T. M. (1983) Zircon saturation revisted: Temperature and composition effects in a variety of crustal magma types. *Earth Planet. Sci. Lett.* **64**, 295–304.

White, A. F. (1995) Chemical weathering rates of silicate minerals in soils. In *Chemical weathering rates of silicate minerals* (eds. A. F. White and S. L. Brantley), pp. 407–461. *Reviews in Mineralogy*, Vol. 31. Mineralogical Society of America, Washington D.C.

White A. F. and Brantley S. L. (1995) Chemical weathering rates of silicate minerals: An overview. In *Chemical Weathering Rates of Silicate Minerals* (eds. A. F. White and S. L. Brantley), pp. 1–22. *Reviews in Mineralogy*, Vol. 31. Mineralogical Society of America, Washington D.C.

White, A. F., Blum, A. E., Schulz, M. S., Bullen, T. D., Harden, J. W. and Peterson, M. L. (1996) Chemical weathering rates of a soil chronosequence on granitic alluvium; I, Quantification of mineralogical and surface area changes and calculation of primary silicate reaction rates. *Geochim. Cosmochim. Acta* **60**, 2533–2550.

White, A. F., Schulz, M., Vivit, D. and Bullen, T. E. (1998) The role of disseminated calcite in rates of calcium release and CO_2 consumption during the weathering of granitoid rocks. *Mineralogical Magazine* **62A**, 1647–1648.

Whitfield, M. (1981) The world Ocean, mechanism or machination. *Interdisciplinary Sci. Rev.* **6**, 12–35.

Whitfield, M. (1982) The salt sea – accident or design? *New Scientist*.

Wood, M. (1995) *Environmental Soil Biology.* 2nd rev. edn. Blackie Academic & Professional, London.

Yeats, P. A. and Bewers, J. M. (1982) Discharge of metals from the St. Lawrence River. *Can. J. Earth Sci.* **19**, 982–992.